

Content: Two tables and seven figures.

Table S1: List of differentially expressed genes in control and *Myt* TF-deficient *Ins*⁺ cells under euglycemic conditions. The presented data on the left columns (C-J) are Log₂(FPKM) of each sample. Column M are fold change without log transform. P-value was calculated using unpaired t-test. The gene list is sorted based their level of increase-to-decrease (from mutant to control cells) from top-to-bottom.

Table S2: Differentially expressed genes between E15.5 islet progenitors and newly born β -cells and their overlap with *Myt* TF-dependent genes in adult β -cells. The gene expression levels were from RNAseq of purified cells NAseq (log₂ transformed FPKM). The expression in E15.5 Neurog3-expressing islet progenitors (column D: average. Columns E-G: three biological repeats) and newly born β -cells (sorted based on β -cell specific eGFP expression. Column I: average. Columns J-L: three biological repeats) are included. For comparison, fold changes (Column C, log₂-transformed) were shown. P-values (column B) were calculated using T-test, two-tailed, type 2 errors. In column (M), genes showing down- or up-regulation in two-months-old *Myt* TF-mutant β -cells (over control β -cells) were noted (as up or down).

Fig. S1. Newly-born *Myt* TF-deficient β -cells produce normal-looking ISGs and have normal glucose response. Islets from P1 mice were isolated via hand-picking. They were then fixed, embedded, and sectioned for TEM studies or directly used for insulin secretion assays. For quantification, ~30 TEM sections (each with 1-3 different β -cell sections). (A, B) Typical ISG morphology in P1 control (A) and *MytPanc* ^{Δ} (B) β -cells revealed by TEM. (C, D) Quantification of ISG density and diameter in P1 control and *MytPanc* ^{Δ} β -cells, respectively. ~30 TEM images with a total of at least 50 whole β -cell areas were quantified by Image J. (E) GSIS of P1 islets in response to basal glucose (2.8 mM, or G2.8), stimulatory glucose (G20), and stimulatory Glucose plus high KCl-induced depolarization (G20 + 25 mM KCl). From (C-E), data are presented as (mean + SEM). Statistical analyses use unpaired student test, all with $p > 0.20$.

Fig. S2. Postnatal islet cells express low-but detectable levels of Neurog 3. IF assays of Neurog3 and Pdx1 in embryonic (E15.5) and P35 pancreas, counter-stained with DAPI, processed side by-side. Note that for visualizing the Neurog3 signals in postnatal islet cells, the Neurog3 signals in most endocrine progenitors were oversaturated. Scale bar=20 μ m.

Fig. S3. *MytPanc* ^{Δ} islets lack significant portions of *Ins*⁺ cells that co-express other hormones. IF assays of Ppy, Sst, Gcg and *Ins* in 4- and 9-week-old islets. Single channels and merged images were shown. Scale bar=20 μ m.

Fig. S4. Lack of *Ins*⁺*Gcg*⁺ or *Ins*⁺*Sst*⁺ cells in recovered allotransplants of *MytPanc* ^{Δ} and control islets (3-months after transplantation). Note that single channels (panels with 2, 3, 4) and merged images (panels with number 1) were shown. To ensure equal multi-hormone+ cell assessments, insulin intensity across different samples were equalized by adjusting confocal parameter (A, B). (C, D) Images showing *Ins* expression levels, captured under identical confocal parameter, highlighting the lower level of insulin in the mutant islets. Scale bar=20 μ m. (E), Random glucose of NSG-DTR mice with/without islet transplantation (~50 IEQs).

Fig. S5. The response of transplanted cells and recipient mice when treated with DT and HFD. (A, B) TUNEL assay of recovered islet transplants from mice receiving DT injection (2-months prior to tissue recovery). (C, D) Weight gain and IPGTT of NSG-DTR mice (transplanted with islets) treated with 3-months of control diet or HFD. Each of these mice received control islet transplantation in one AEC and mutant islets in the other. Note that one mouse was not used for following up analysis (red arrow in C) because of low weight gain. P is from Two-way ANOVA, with repeated measures. Scale bars, 20 μ m.

Fig. S6. The efficacy of *Rip*^{Cre-TG}-mediated gene deletion. (A-C) Cre-activity assay in β -cells of *Rip*^{Cre-TG}; R26ReYFP mice. (A, B) Two islet examples were included to demonstrate the heterogenous nature of Cre-expression. (C) Portion of Ins⁺ cells that co-express eYFP (mean + SEM). (D, E) IF showing co-expression of Pdx1 (red) and Myt TFs (green). In this case, antibodies against Myt1, Myt2, and Myt3 signals were labeled as the same color (green). Note that all Pdx1⁺ cells have Myt TF signals in controls but not mutants. (F) IPGTT of mutant and control mice at 3-months of age (both males and females). 1 g/kg glucose dosage were used. In controls, both WT and *Rip*Cre^{TG} mice were included. *: p<0.05, unpaired type 2, two-tailed t-test. (G, H) Random glucose and total insulin in control and *Myt* $\beta\Delta$ mice (p=0.09 in H, t-test). (I, J) TUNEL staining in 2-months old *Myt* $\beta\Delta$ and control islets. Note the presence of a TUNEL-signal⁺ cell that does not express insulin (I, arrow), acting as a positive control of the assay. Scale bars=20 μ m.

Fig. S7. Myt TF-deletion efficacy in eYFP⁺ cells. cDNA reads of *Myt3* overlaid to the genomic sequence. *Myt3* exons are marked with blue rectangles. Three controls (C1, C2, C3) and two mutants (M1, M2) were shown. Note that the reads covering the floxed exons (marked with red bars) of *Myt1*, *Myt2*, and *Myt3* were mostly gone in the mutant samples. The residual reads of these escaper exons, relative to their flanking exons, were used to calculate the efficacy of Myt TF deletion in the *Rip*^{Cre-TG}-active cells.

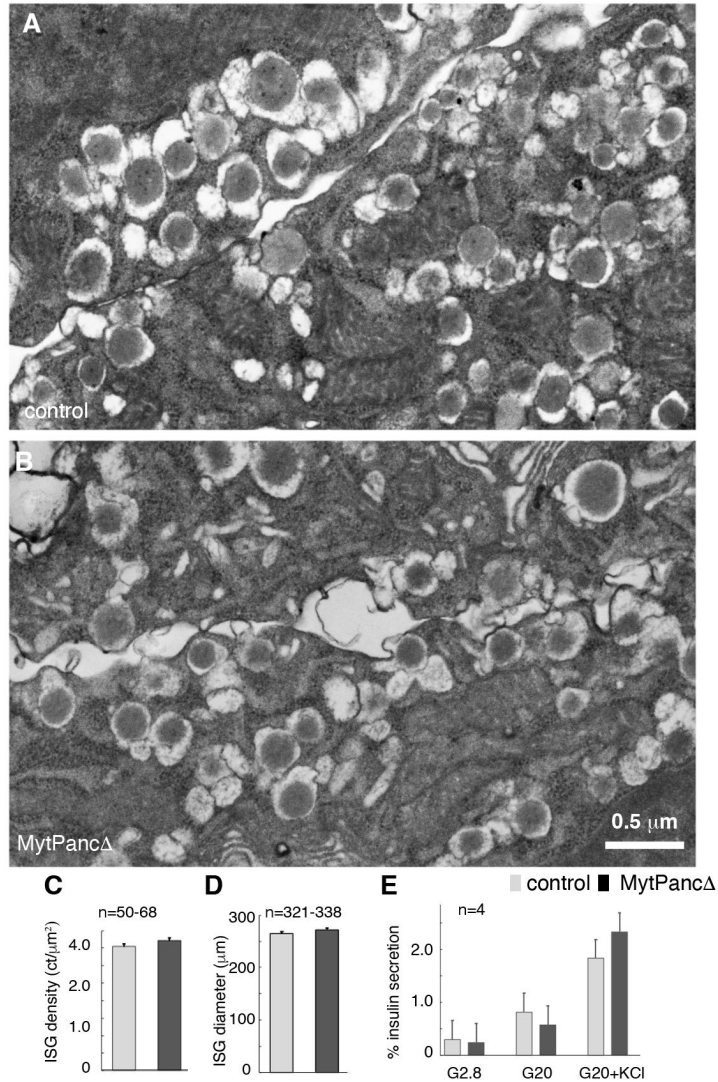


Fig. S1. Newly-born Myt TF-deficient β-cells produce normal-looking ISGs and have normal glucose response. Islets from P1 mice were isolated via hand-picking. They were then fixed, embedded, and sectioned for TEM studies or directly used for insulin secretion assays. For quantification, ~30 TEM sections (each with 1-3 different β-cell sections). (A, B) Typical ISG morphology in P1 control (A) and *MytPanc^Δ* (B) β-cells revealed by TEM. (C, D) Quantification of ISG density and diameter in P1 control and *MytPanc^Δ* β-cells, respectively. ~30 TEM images with a total of at least 50 whole β-cell areas were quantified by Image J. (E) GSIS of P1 islets in response to basal glucose (2.8 mM, or G2.8), stimulatory glucose (G20), and stimulatory Glucose plus high KCl-induced depolarization (G20 + 25 mM KCl). From (C-E), data are presented as (mean + SEM). Statistical analyses use unpaired student test, all with $p > 0.20$.

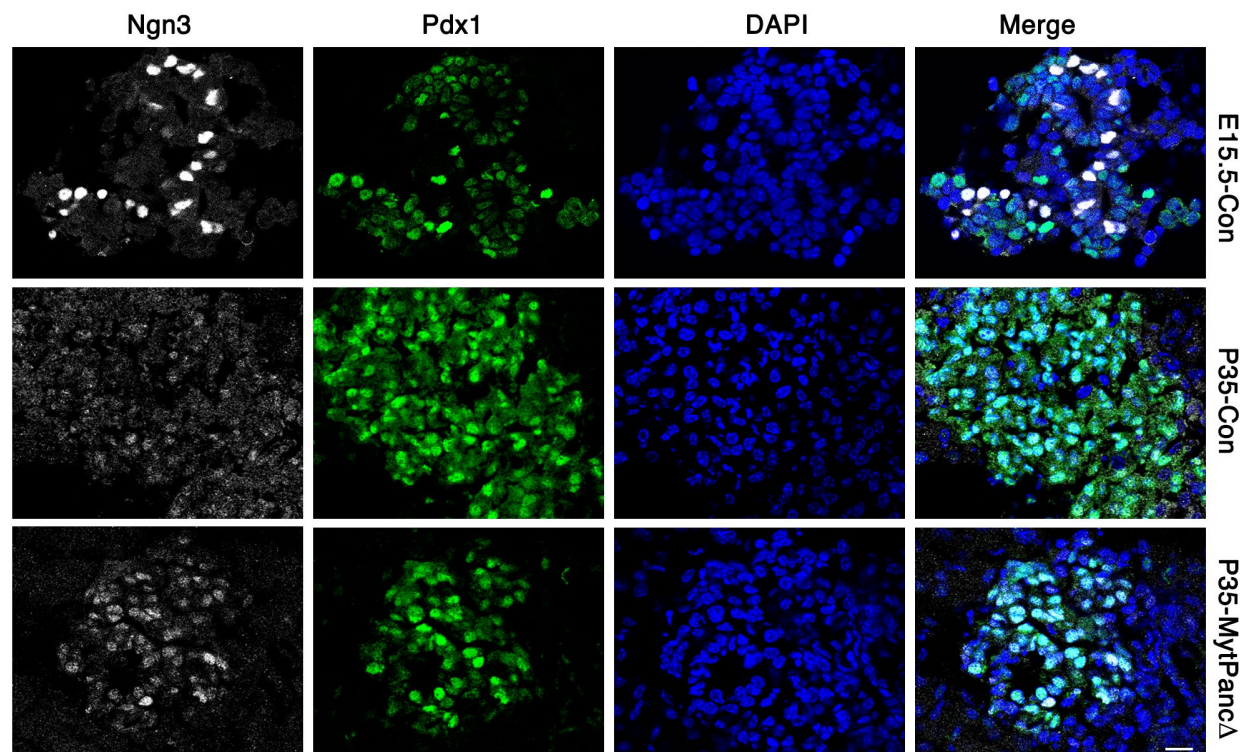


Fig. S2. Postnatal islet cells express low-but detectable levels of Neurog 3. IF assays of Neurog3 and Pdx1 in embryonic (E15.5) and P35 pancreas, counter-stained with DAPI, processed side by-side. Note that for visualizing the Neug3 signals in postnatal islet cells, the Neurog3 signals in most endocrine progenitors were oversaturated. Scale bar=20 μ m.

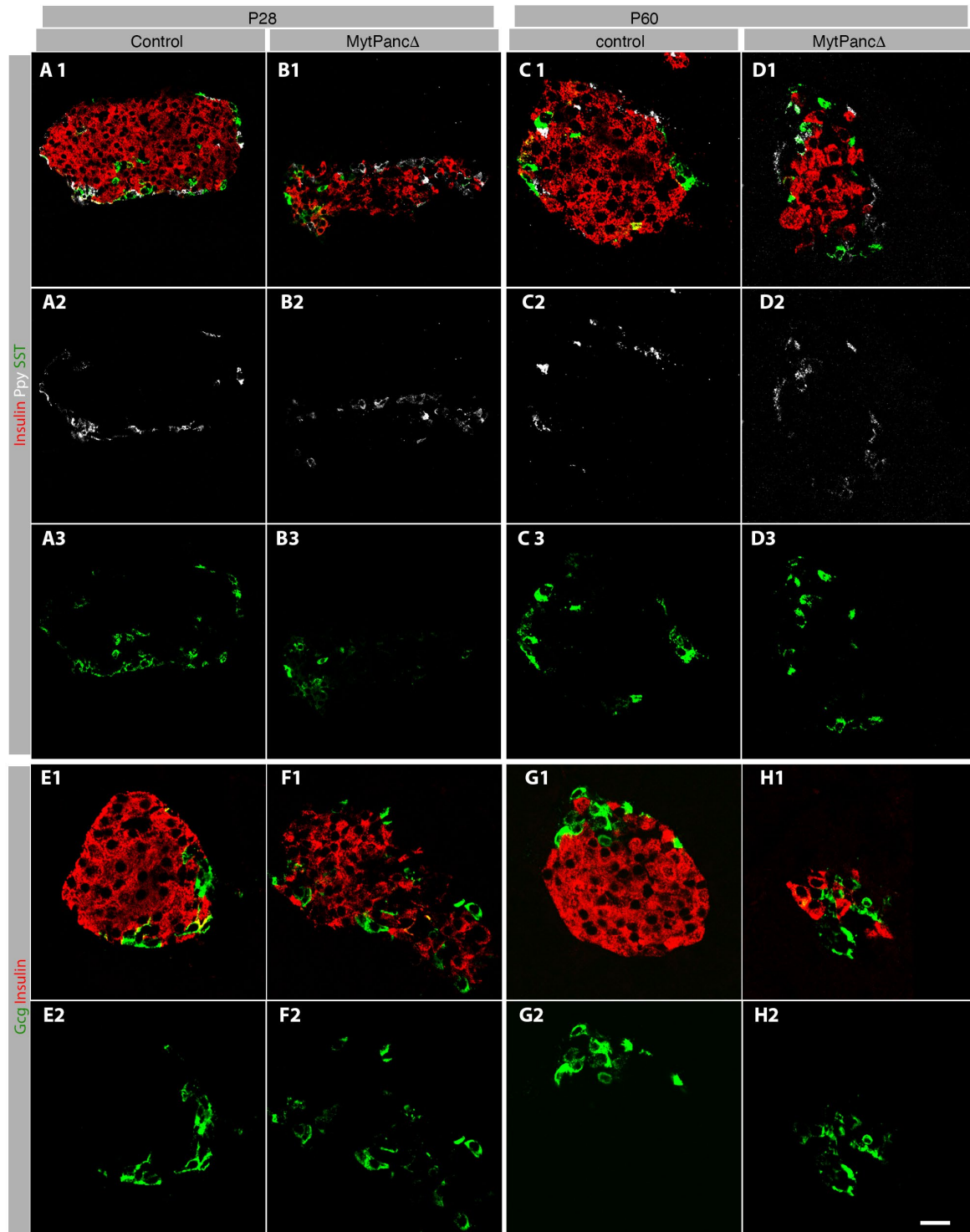


Fig. S3. *MytPanc*^Δ islets lack significant portions of Ins⁺ cells that co-express other hormones. IF assays of Ppy, Sst, Gcg and Ins in 4- and 9-week-old islets. Single channels and merged images were shown. Scale bar=20 μ m.

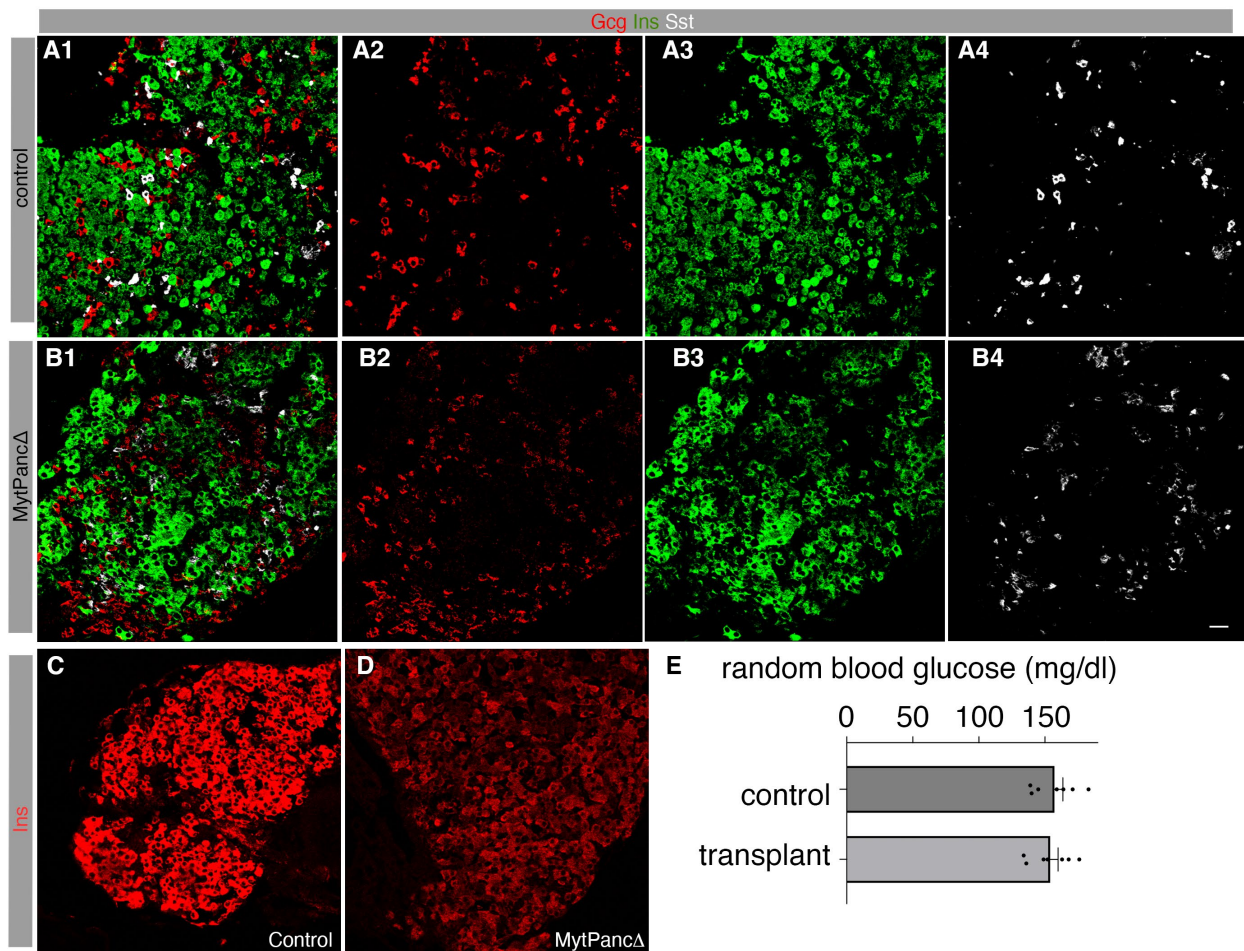


Fig. S4. Lack of Ins^+Gcg^+ or Ins^+Sst^+ cells in recovered allotransplants of *MytPancΔ* and control islets (3-months after transplantation). Note that single channels (panels with 2, 3, 4) and merged images (panels with number 1) were shown. To ensure equal multi-hormone+ cell assessments, insulin intensity across different samples were equalized by adjusting confocal parameter (A, B). (C, D) Images showing Ins expression levels, captured under identical confocal parameter, highlighting the lower level of insulin in the mutant islets. Scale bar=20 μm . (E), Random glucose of NSG-DTR mice with/without islet transplantation (~50 IEQs).

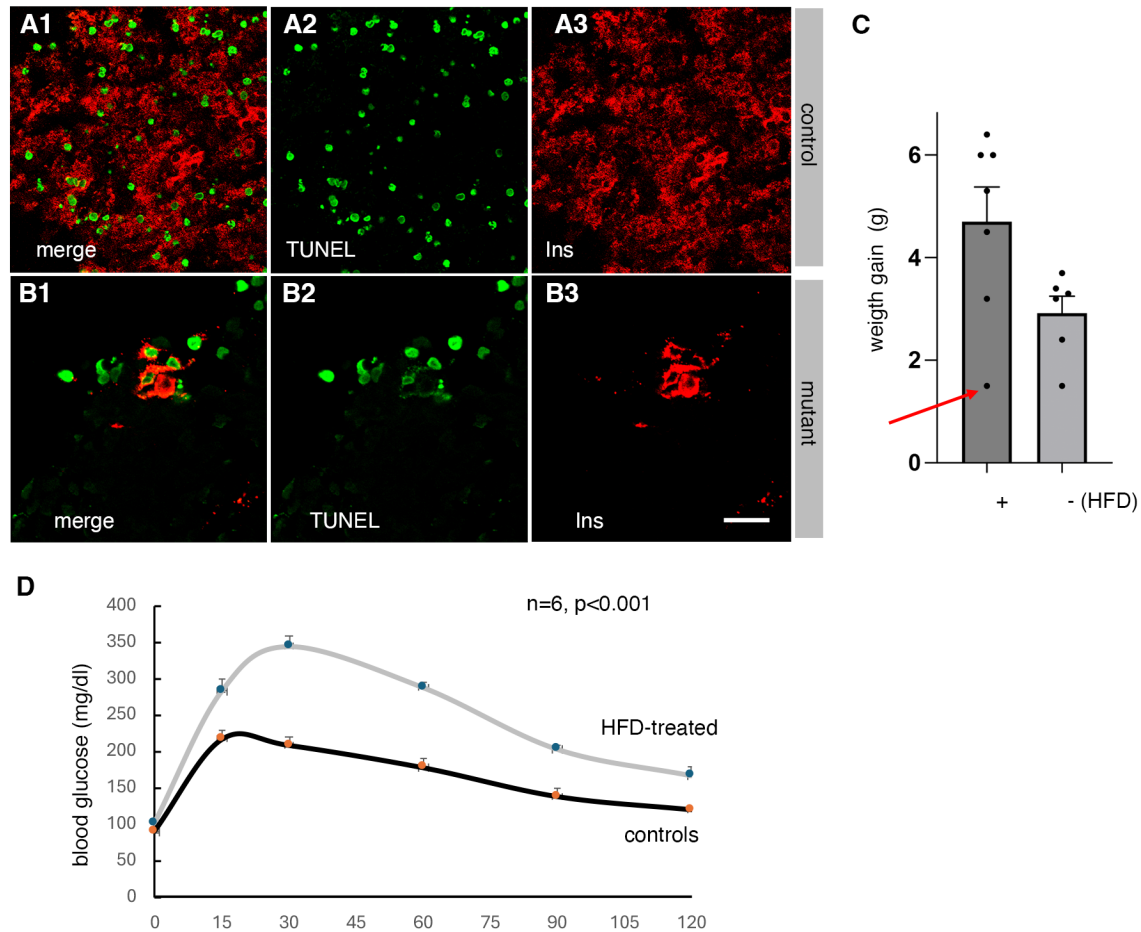
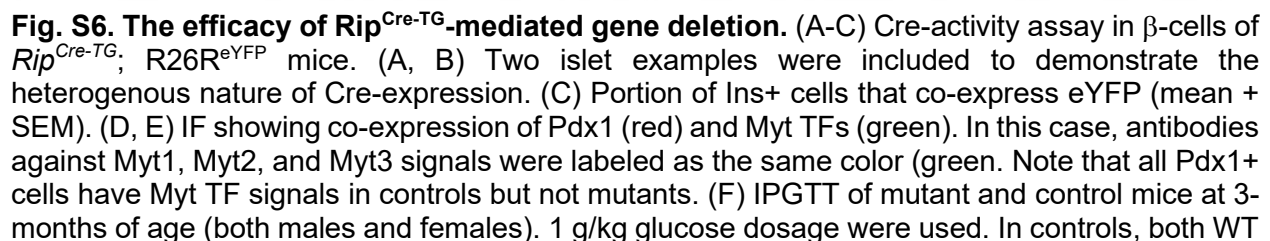


Fig. S5. The response of transplanted cells and recipient mice when treated with DT and HFD. (A, B) TUNEL assay of recovered islet transplants from mice receiving DT injection (2-months prior to tissue recovery). (C, D) Weight gain and IPGTT of NSG-DTR mice (transplanted with islets) treated with 3-months of control diet or HFD. Each of these mice received control islet transplantation in one AEC and mutant islets in the other. Note that one mouse was not used for following up analysis (red arrow in C) because of low weight gain. P is from Two-way ANOVA, with repeated measures. Scale bars, 20 μ m.



and *RipCre*^{TG} mice were included. *: $p < 0.05$, unpaired type 2, two-tailed t-test. (G, H) Random glucose and total insulin in control and *Myt $\beta\Delta$* mice ($p = 0.09$ in H, t-test). (I, J) TUNEL staining in 2-months old *Myt $\beta\Delta$* and control islets. Note the presence of a TUNEL-signal⁺ cell that does not express insulin (I, arrow), acting as a positive control of the assay. Scale bars=20 μm .

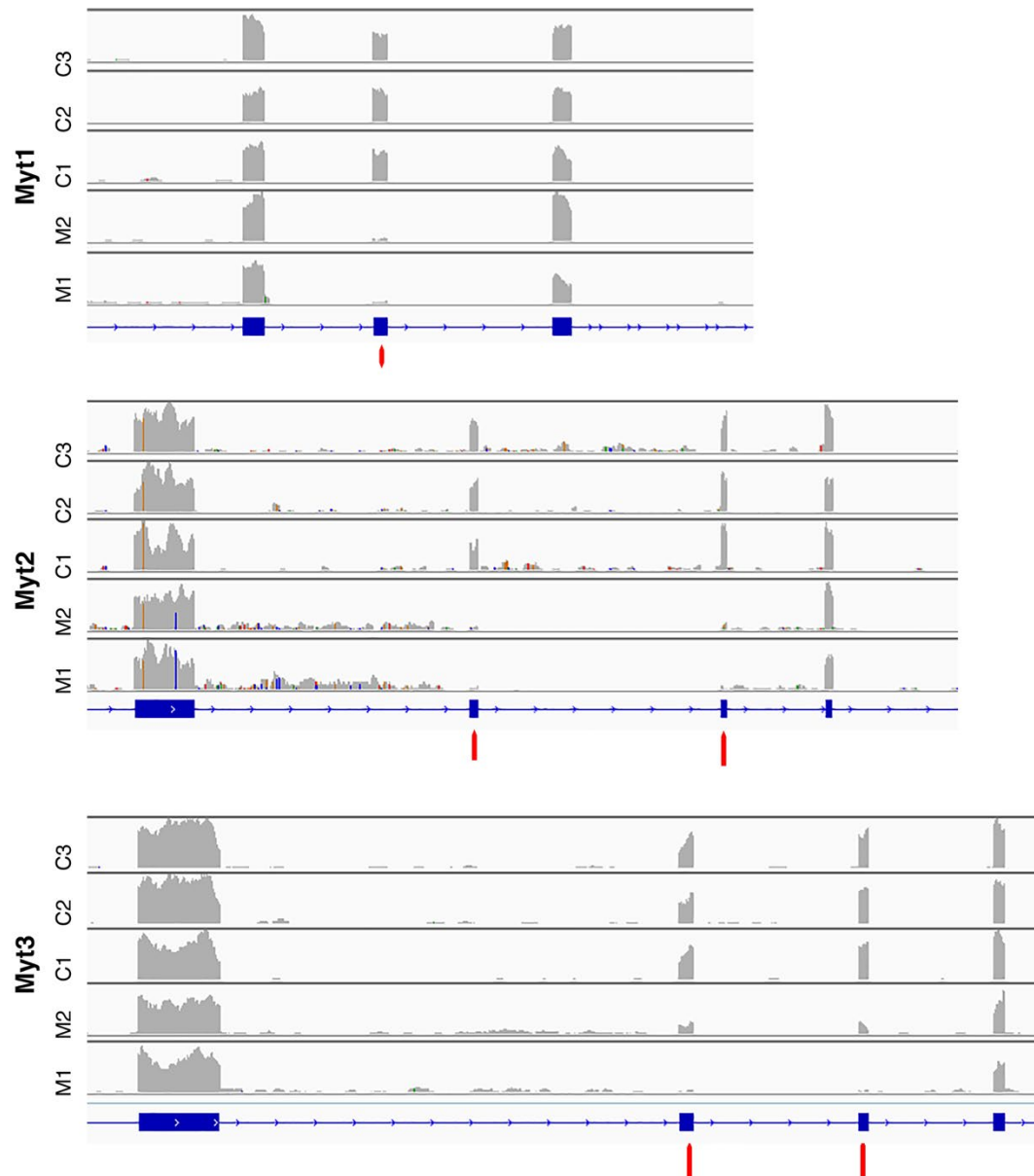


Fig. S7. Myt TF-deletion efficacy in eYFP⁺ cells. cDNA reads of *Myt3* overlaid to the genomic sequence. *Myt3* exons are marked with blue rectangles. Three controls (C1, C2, C3) and two mutants (M1, M2) were shown. Note that the reads covering the floxed exons (marked with red bars) of *Myt1*, *Myt2*, and *Myt3* were mostly gone in the mutant samples. The residual reads of these escaper exons, relative to their flanking exons, were used to calculate the efficacy of Myt TF deletion in the *Rip*^{Cre-TG}-active cells.